American Mineralogist, Volume 83, pages 316–322, 1998

Reactions of aqueous Au^{1+} sulfide species with pyrite as a function of pH and temperature

M.J. Scaini, G.M. Bancroft, and S.W. Knipe

Department of Chemistry, University of Western Ontario, London, Ontario N6A 5B7, Canada

Abstract

The reactivity of aqueous Au^{1+} sulfides with FeS_2 at pH = 3 and 6 for temperatures of 25 and 90 °C has been investigated using X-ray photoelectron spectroscopy (XPS), scanning electron microscopy with energy dispersive X-ray analysis (SEM/EDXA), and static secondary ion mass spectrometry (SSIMS). The presence of both Au^{1+} and metallic Au are observed upon the FeS_2 surface. We show that Au deposition is increased at elevated pH or temperature; but the amount of Au deposited is far lower than in $AuCl_4^-$ solutions owing to the greater stability of $Au(SH)_x^{1-x}$ complexes. This is the first evidence of Au^{1+} on pyrite from bisulfide solutions using XPS.

Introduction

It is generally accepted by the geologic community that the bisulfide ligand (SH^-) plays an important role in the transport of precious metals, and SH^- is believed to be the principle transporting species when both chloride and bisulfide ligands are present in solution in significant quantities (Hayashi and Ohmoto 1991). When considering the bisulfide ligand as a complexing agent in aqueous and hydrothermal environments, researchers have focused on two areas. First, several researchers have studied the ability of the ligand to complex various precious metals such as Au (Renders and Seward 1989a; Shenberger and Barnes 1989; Seward 1993; Berndt et al. 1994; Benning and Seward 1995, 1996), Ag (Renders and Seward 1989a; Gammons and Barnes 1989), Pt and Pd (Gammons and Bloom 1993; Wood et al. 1994; Pan and Wood 1994). They determined (1) the solution species present as a function of temperature, pressure, or pH and (2) the maximum solubility of the metals to better understand transport resulting in ore deposition. Second, geologists and hydrometallurgists have focused on the interaction of base metal sulfides and bisulfide solutions with the hope of better understanding base metal ore deposition, oxidation/reduction processes, and base metal recovery (Hayashi et al. 1990; Buckley et al. 1994; Kucha et al. 1994).

Renders and Seward (1989b) first investigated the interactions of Au^{1+} bisulfide and sulfide minerals. They investigated the ability of synthetic antimony and arsenic sulfides (Sb_2S_3 and As_2S_3) to adsorb Au from bisulfide solutions as a function of pH and temperature. These minerals were chosen owing to high Au concentrations found in the hydrothermal deposits of New Zealand. This study was later followed up by Cardile et al. (1993), who used ^{197}Au Mössbauer to characterize the oxidation state of the Au present on the As_2S_3 and Sb_2S_3. It was concluded that the Au was present on the surface as a Au^{1+} species. It was postulated that the Au was in the form of a linear complex attached to the sulfide surface through the sulfur moiety [S—Au^{1+}-SH^-]. Tossell (1996) has calculated the IR-Raman vibrational frequencies and the ^{197}Au Mössbauer parameters for a variety of hydrothermally relevant Au^{1+} and Au^{3+} species. Tossell (1996) has also shown that the Au^{1+} sulfide can be adsorbed onto an antimony sulfide surface as the AuSH neutral species through the sulfur of the sulfide mineral, in good agreement with the experimental observations of Cardile et al. (1993).

This work focuses on the first surface studies of Au^{1+} sulfide complexes on pyrite as a function of pH and temperature from bisulfide solutions. Information on oxidation state, surface coverage, and morphology of the deposited Au species obtained is discussed through the use of XPS and SEM/EDXA.

Experimental materials

Pyrite was cut into 10 × 5 × 5 mm slabs for use in the experiments. Ultra-high purity Ar and H_2S gases from Matheson gas were used. All other reagents were of high purity and used as received (BDH chemicals). The Au_2S was prepared following the procedure outlined by Renders and Seward (1989a).

Experimental procedure

The bisulfide solution was prepared by taking 175 mL of freshly prepared 0.20M NaOH, and placing it into a blackened 250 mL three-neck flask. To the center neck of the flask, a water-cooled condenser was added. The temperature was adjusted using a variable transformer that had been calibrated, thus allowing for temperatures to be within ±1 °C of the chosen 25 or 90 °C. In the two smaller necks of the flask, a gas bubbling frit and gas exhaust line were added. This allowed the system and the solution to be purged with ultra-high purity argon gas.

The argon gas was passed through a scrubbing column

0003–004X/98/0304–0316$05.00

30 cm in length which was packed with BASF R3-11 scrubbing catalyst to remove any possible O_2. The argon purge was maintained for 1 h. Then a T-valve was turned and H_2S was allowed to flow into the system. The H_2S was also purged for 1 h. During the gas purging, the solutions were continuously stirred. After the 1 h H_2S purge, the gas bubblers were pulled from the solution and the gas flow was switched back to argon. This allowed the argon gas to flow over the surface of the solution and prevent any backstreaming of the atmosphere into the reactors.

The gas exhaust line was temporarily removed and the pH electrode was placed into the solution. The pH was measured using an Orion model SA 720 pH meter with a Radiometer America pH electrode (GK 733526). The pH was then adjusted to the chosen value, either 3.0 or 6.0 (using HCl or NaOH). Once the pH had been adjusted, the gas exhaust line was replaced and the temperature adjusted to the desired value. Once the system had reached the desired temperature, and with the argon gas still flowing over the solution, solid Au_2S (30 ±2 mg) was added to the flask.

The system was left stirring for 1 h prior to pyrite insertion. The polished pyrite plates (same polishing protocol as described in Scaini et al. 1995) were secured into PTFE holders with a nylon screw and then placed into the neck that previously contained the gas exhaust line. Samples were reacted for a period of either 1 d or 1 week. Samples were oriented to minimize the amount of Au_2S solid adsorbing onto the pyrite surfaces. At the end of the reaction, the condenser was removed and replaced with a glass stopper.

The reaction flasks were then placed into a glove bag to allow for the removal of the reacted pyrite samples in an inert atmosphere. After sealing the bag, a series of five fill and purge cycles were performed with argon gas before removing the samples from solution. The room lights were turned off and a small desk lamp was then used to illuminate the glove bag. The reacted pyrite plates were removed from the bisulfide solution, rinsed with doubly distilled, deionized water and analytical grade methanol before mounting on the analysis holder. Once the samples were secured to the holder, it was then placed into a darkened glass vessel and sealed for transport to the XPS spectrometer. The sealed vessel was then placed into another glove bag attached to the X-ray spectrometer, and a series of five fill and purge cycles were performed before opening the vessel and introducing the sample into the spectrometer. Surface analysis of the reacted pyrite samples was done using the procedures and parameters previously discussed in detail by Scaini et al. (1995).

Static SIMS was performed on a ZAB-2f spectrometer. The primary ion source was a Gallium metal ion gun at 25 kV, 60 pA primary ion current with the instrument run in negative ion mode to increase the sensitivity toward Au and S. Secondary electron microscopy was performed on either a Hitachi S-4500 series Field Emission microscope or an ISI-DS 130 microscope with attached energy dispersive X-ray analyzer.

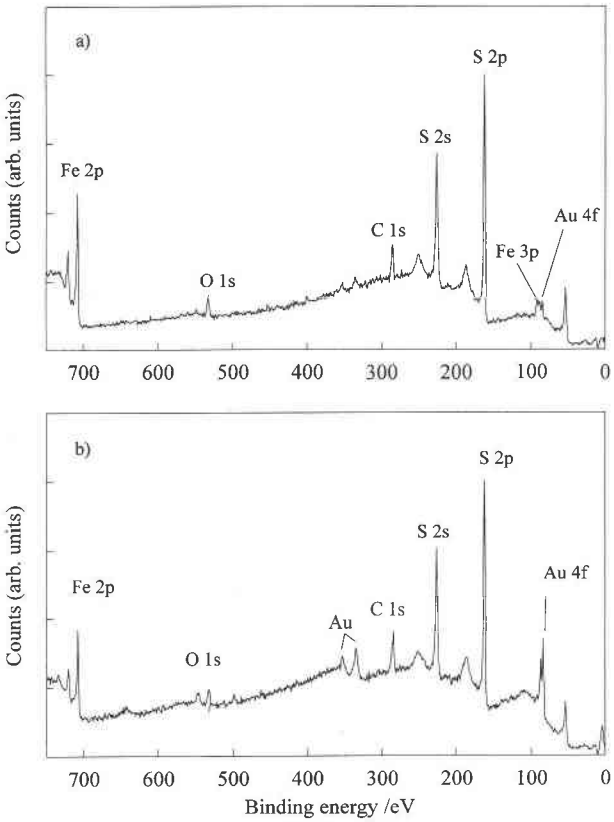

Figure 1. XPS broadscans of 1 week reacted pyrite samples at pH = 3.0 in black flasks at (**a**) 25 °C and (**b**) 90 °C.

Atomic absorption analysis

A Varian Spectraa-10 Atomic Spectrometer, with an air-acetylene gas supply was used. The entire 175 mL of the gold sulfide solution was reacted with 40 mL of H_2O_2 and 60 mL of concentrated HNO_3, after filtration through a fine sintered glass funnel. The solution was then evaporated until dry. The solid residue was then dissolved in 15 mL aqua regia and diluted to 50 mL total volume.

Results and discussion

Identification of adsorbed Au^{1+}

Figure 1 shows the broadscan surveys from pyrite samples reacted for 1 week at pH = 3.0 and at 25/90 °C. There are two important features shown in Figure 1. First, the amount of Au present on pyrite from bisulfide solution after 1 week is very small, especially when compared to the chloride systems (Mycroft et al. 1995; Scaini et al. 1997). The amount of Au present upon the surface according to XPS broadscan analysis is <1 at% (Fig. 1a), and no more than 3% (Fig. 1b) even after a 1 week exposure; whereas in previous studies with $AuCl_4^-$, the surface Au concentrations are approximately an order of magnitude higher. It is not until Au concentrations in

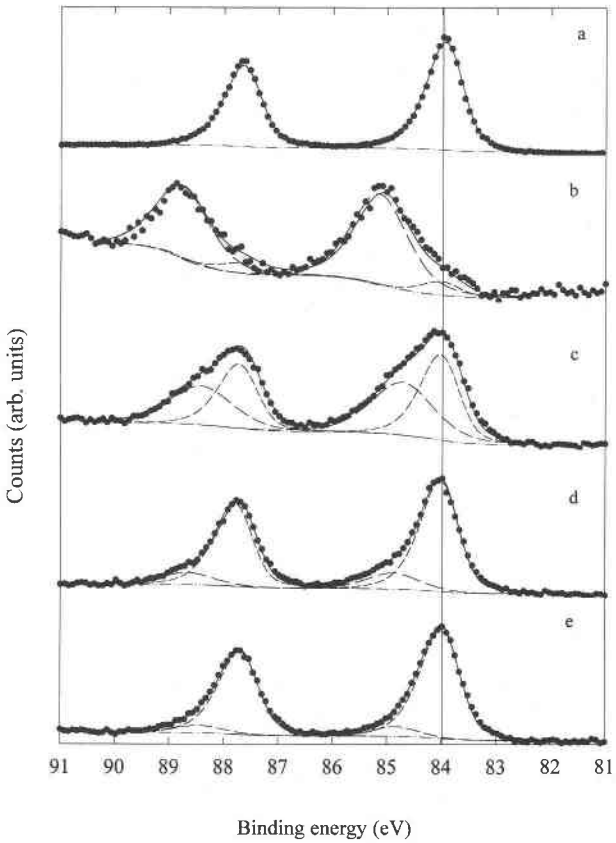

FIGURE 2. Au 4f narrow region surveys for (**a**) pure metallic Au (**b**) and (**c**) 1 d reaction at 25 °C, black flask (**d**) 1 d reaction at 90 °C, black flask and (**e**) 1 d reaction at 90 °C clear flask. All reacted pyrite samples were run at pH = 3.0.

$AuCl_4^-$ solutions decrease to $\sim 10^{-6}$ M that similar low Au surface concentrations are observed and even in those cases the time frame for the reaction is only 1 d, not 1 week. Second, the Au 4f intensity increases greatly from 25 to 90 °C. The effect of temperature upon the uptake of Au is discussed later.

To determine the oxidation state of any Au species present on the pyrite surfaces, narrow scan Au 4f spectra were recorded (Fig. 2). Table 1 summarizes the Au $4f_{7/2}$ XPS peak positions. At 25 °C, (Figs. 2b and 2c), the Au $4f_{7/2}$ peaks are broad and shifted by about 1 eV compared to the bulk Au metal signal (Fig. 2a). Compared to any previous spectra with $AuCl_4^-$ reacted with pyrite (Mycroft et al. 1995) these high binding energy peaks are relatively much more intense and somewhat broader. High binding energy Au 4f shoulders are also present at 90 °C (Figs. 2d and 2e in black and clear flasks, respectively), but clearly the majority of the Au is present as bulk Au metal in these two cases.

The intense high binding energy peak at ~85 eV in Figures 2b and 2c is mostly due to a Au^{1+} sulfide species. These peaks could also be, at least partly, due to small Au metal clusters (5–7 atoms) that give a Au $4f_{7/2}$ binding energy up to 84.7 eV (Dicenzo et al. 1988; Mycroft et al. 1995), which then shifts toward the bulk Au value of 84.0 eV as the size of the cluster increases. The Au $4f_{7/2}$ peak at 85.1 eV (Fig. 2b) is at too high a binding energy for small-particle Au. But, in addition, a small particle interpretation implies that this surface is almost entirely covered with very small clusters (Mycroft et al. 1995). However, as seen in the SEM micrographs of these surfaces (Fig. 3a) there are significant numbers of large Au clusters, which indicate a distribution of Au particle sizes.

TABLE 1. Au $4f_{7/2}$ binding energies for the second fitted peak from gold-reacted pyrite samples

Figure 2	Au $4f_{7/2}$ (eV)	Peak width (eV)
b	85.1	1.3
c	84.9	1.2
d	84.8	1.1
e	84.7	1.0

The Au $4f_{7/2}$ binding energy of Au^{1+} S adsorbed species agrees with the value expected from model compounds. Van de Vondel et al. (1977) used XPS to study various compounds in which Au is bound to two S atoms in a linear fashion (S-Au-S). They reported Au $4f_{7/2}$ binding energies of 85.0 and 85.2 eV (relative to C 1s = 285.0 eV). The structure of these compounds is similar to that proposed by Cardile et al. (1993) to explain their Mössbauer results for the interaction of Au^{1+} bisulfide solutions with Sb_2S_3 and As_2S_3, where one sulfur atom is from the substrate while the other is from the bisulfide ligand. Clearly, the majority of species in Figure 2b are adsorbed Au-S. The change in the relative intensity of the high binding energy peak (Figs. 2d, 2e) is understandable since as one increases the temperature, the sticking coefficient may be reduced, allowing for easier desorption back into solution. The higher temperature may also help overcome the bond energy between Au^{1+} and the bisulfide ligand allowing for a more rapid reduction of the Au^{1+} to Au. These single Au atoms could then in turn migrate across the surface to form larger aggregates.

Based upon the Au narrow region alone, no one single explanation seems to entirely satisfy the criteria needed to explain peak position and width. There must be a mixture of Au^{1+} and both small particles and bulk Au metal on the FeS_2 surface from bisulfide solution. For example, the differences between Figures 2b and 2c are difficult to reconcile. Because the solution conditions were reproduced (pH = 3.0, 1 d reaction, 25° C), this dramatic difference is quite unexpected.

One possible mechanism is that the second sample dissolved more rapidly than the first. The released Fe^{2+} could reduce the Au^+ more rapidly, both in solution and at the surface. Another possible explanation may be photoreduction of the adsorbed Au bisulfide. In some cases, a PTFE sample holder became stuck in the flask. This resulted in a longer period of time during which the removed samples sat exposed to light (from the desk lamp). For example, it was possible to take a sample (stored in the dark) that had a spectrum similar to that of Figure 2b,

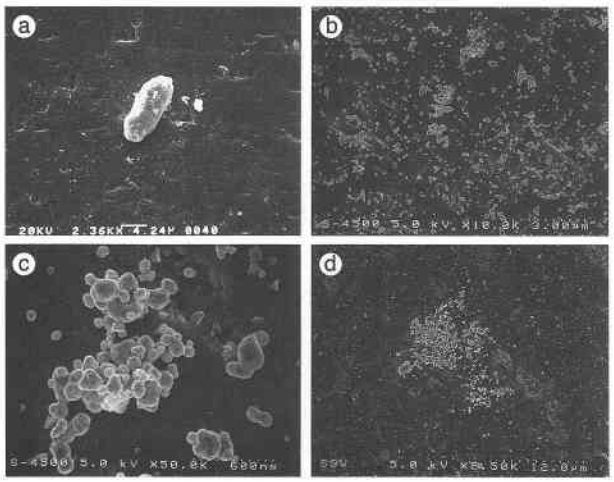

FIGURE 3. SEM micrographs of 24 h reacted FeS_2 at (**a**) pH = 3.0, 25 °C, (**b**) and (**c**) pH = 3.0, 90 °C, and (**d**) pH = 6.0, 90 °C.

analyze it several months later, and observe a Au 4f spectrum similar in peak shape found in Figure 2c. Clearly, the $Au^{1+}SH$ complex is not stable with respect to surface reduction.

Other evidence to support the possibility of an adsorbed Au^{1+} bisulfide may come from the evaluation of the S 2p region. Figure 4 shows the S 2p region of fractured and Au bisulfide reacted pyrite samples. The assignment of species has been previously discussed Mycroft et al. (1995). As seen in the spectra, the low and high binding energy peaks increased after reaction, indicating an increase in the mono- and polysulfide species on the surface. The work of Leavitt and Beebe (1994), on the interactions of H_2S with the (111) surfaces of Au, revealed that the S 2p binding energy when H_2S is adsorbed on Au is 163.0 eV and that of SH^- is 162.4 eV, relative to C 1s at 285.0 eV. Therefore, if SH^- is adsorbed or bonded to the Au on the mineral surface, no discernible changes in the S 2p spectrum would become evident because the SH^- peaks are at the same B.E. as the substrate FeS_2 S 2p peaks. This fact was also born out experimentally when comparing pyrite samples that reacted in bisulfide solutions with and without the added Au complex, and no differences in peak shape or position were observed.

To obtain more conclusive evidence of the existence of the adsorbed Au^{1+} bisulfide on the pyrite surface, static secondary ion mass spectrometry (SSIMS) was performed on some of the reacted samples. Figure 5 is a series of mass spectra for a variety of gold and pyrite samples. If AuSH exists on the surface, then observation of mass fragments corresponding to AuS (229) and AuSH (230) would be expected. In Figure 5a, the mass of 197 (Au) along with masses 229 (AuS) and 230 (AuSH) are observed from pyrite reacted in the Au containing bisulfide solution. However, a side effect of SIMS analysis is the recombination of ion fragments before detection.

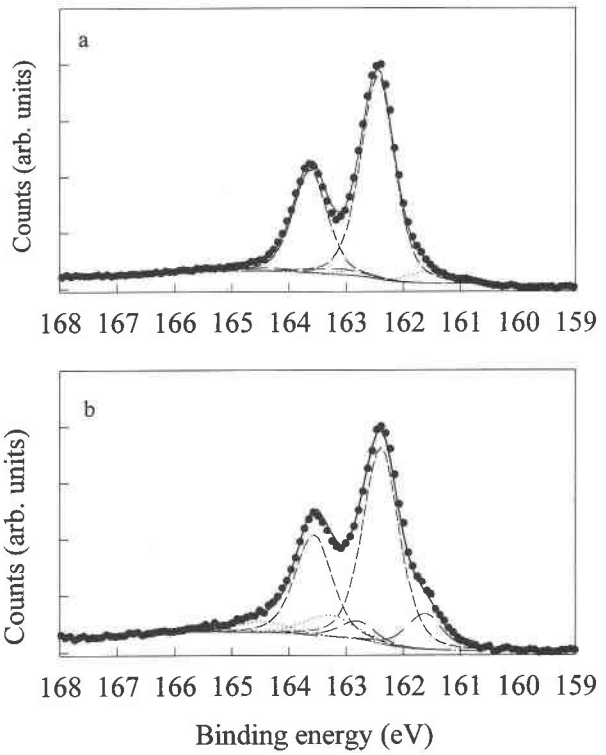

FIGURE 4. S 2p narrow scans of (**a**) in vacuo fracture and (**b**) 24 h reaction at pH = 3.0, 25 °C.

SSIMS tries to minimize this problem through the use of lower beam energies and ion fluxes.

Recombination was tested for by analyzing a Au reacted pyrite sample (Au = 10^{-6}M, pH = 3.0, Cl^- = 1.0M), where bisulfide had not been used (Fig. 5b). Again the mass signals at 229 and 230 are clearly observed. An Au-sputter coated pyrite sample was produced and analyzed (Fig. 5c). The mass responses observed at 229 and 230 clearly support the hypothesis that recombination has occurred above the mineral surface before the mass fragments reached the detector, prohibiting the easy use of SSIMS to confirm adsorbed Au^{1+} bisulfide.

Effect of pH and temperature

Upon comparison of the data in Table 2, there is no increase in surface Au (at longer reaction times); indeed there may actually be a decrease in the Au uptake by the pyrite substrate when comparing the reactions at either pH or temperature. Although the data at pH = 3 and 90 °C shows a very slight decrease in the Au:S ratio, the data at pH = 6, 90 °C show a more marked decrease in the ratio when comparing the 1 d and 1 week samples. If this decrease is real, then some possible explanations are: (1) an increase in substrate dissolution or (2) remobilization of metallic Au from the surface back into solution. If an increase in mineral dissolution is occurring, the presence of Fe in solution would be expected. AA analysis has confirmed the presence of Fe in solution.

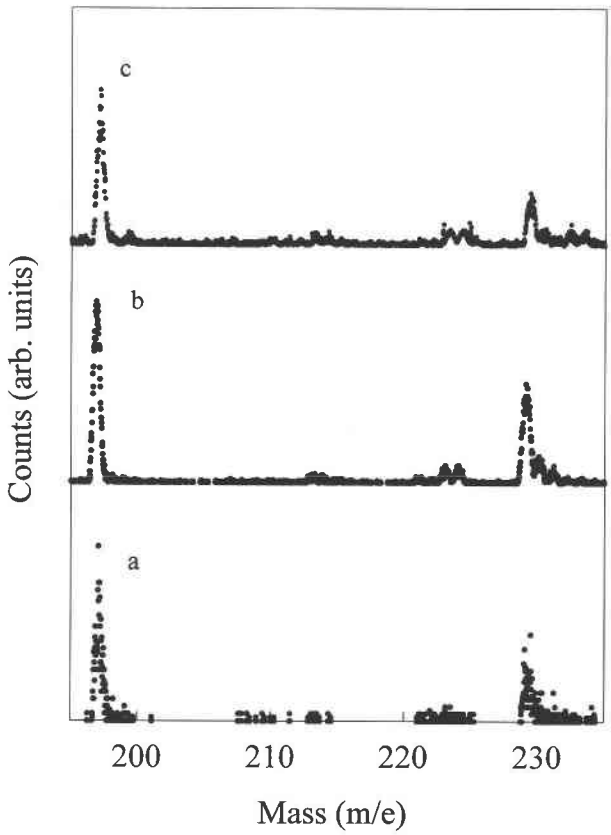

Figure 5. Static SIMS analysis of pyrite samples reacted in (**a**) bisulfide solution, pH = 3.0, 25 °C, black flack (**b**) 1×10^{-6} M Au in 1.0M NaCl at pH = 3.0 and (**c**) Au sputter coated sample.

Analysis from 1 week, pH = 3.0 reactions has revealed the presence of up to 9.7 ppm Fe in the original 175 mL volume (or 9.8×10^{-4} mol/L). The increase in mineral dissolution can also be seen visually in the SEM images of Figure 3.

The effect of pH and temperature upon the uptake of Au by the pyrite samples is clearly seen (Table 2). When comparing the different pH results at 25 °C and 1 d reaction time, the difference in the Au:S ratio is quite dramatic. According to Renders and Seward (1989a), the principle species at acidic conditions is the neutral AuSH; while under near-neutral pH values the anionic form, $Au(SH)_2^-$ is thought to be the dominant species. From their work, the Au^{1+} complex has its greatest solubility at approximately pH = 7. Thus, as one approaches maximum solubility more Au is expected in the solution. This in turn allows for more Au to be adsorbed and subsequently reduced, and is born out by the Au:S ratio being approximately 1 order of magnitude larger at the higher pH at 25 °C. However this conclusion is a little more difficult to reach for the 1 week reactions. Although the data for the 1 week reactions does show an increase, the increase in Au uptake is not as large.

Temperature as well has an effect upon the uptake, producing Au:S ratios larger at 90 °C, in some cases at least an order of magnitude greater than at 25 °C (Fig. 1). Several possible explanations for this may be valid. First, as the temperature is increased, the adsorbed Au^{1+} complex undergoes loss of its coordinating ligand more readily allowing for more Au^{1+} to be adsorbed from solution and a greater rate of reduction on the pyrite surface. However, this increase in thermal energy could also result in less Au on the surface from an enhanced rate of desorption and a decrease in solution dielectric constant that leads to an increased Au-ligand bond strength. Second, there is the possibility that more Au has gone into solution from the starting composition Au_2S (Seward 1973), and this results in an increase in adsorption and reduction rates. Third, disproportionation of Au_2S could proceed more rapidly at 90° C, giving colloidal Au in solution and at the surface. Last, with the increase in temperature, solubility of the FeS_2 substrate is increased, releasing more Fe^{2+} into solution to interact with the Au^{1+} species. The end result is formation of more metallic Au and Fe^{3+}.

Table 2. Atomic Au:S ratios for reacted pyrite samples in bisulfide solution

	pH = 3		pH = 6	
Days	25 °C	90 °C	25 °C	90 °C
1	0.005(2)	0.11(4)	0.03(2)	0.16(6)
7	0.004(2)	0.08(3)	0.01(6)	0.07(4)

Note: Standard deviations in brackets are from three duplicate measurements. Data obtained from XPS broadscan surveys.

Figure 3 shows a series of SEM images of a pyrite reacted for 1 d. The large growth in the center of Figure 3a has been verified by EDXA to be Au (Fig. 6a). From inspection of Figure 3a, it becomes clear that the surface is covered with many very small growths. The composition of the small growths, is also Au, as verified by EDXA (Fig. 6b). Figures 3b and 3c are a pair of SEM images for pyrite samples reacted for 1 d at pH = 3.0 and 90 °C. That the size of the particles is much larger at 90 °C than at 25 °C becomes apparent upon comparing the SEM images. The surface coverage also appears to be higher (as verified by XPS analysis (Fig. 1) Both of the images also illustrate a high degree of surface modification (many etch pits) and particles. In Figure 3d (pH = 6.0, 90 °C), the degree of etching has increased even further and is linked to the increase in the pH and temperature. One can also see many clusters present upon the surface. In all of the SEM images, the Au morphology appears to be spherical, with some of the crystals having slightly more structure (Fig. 3c). The crystals appear to have altered octahedral faces. These structures are in good agreement with those obtained by Lawrance and Griffin (1994) (Figs. 3b, 3e, 5c, and 5d in their paper) who obtained crystals in natural samples ranging from octahedra to polycrystalline aggregates.

The amount of Au found on samples reacted for this time period is much less than that obtained from similar

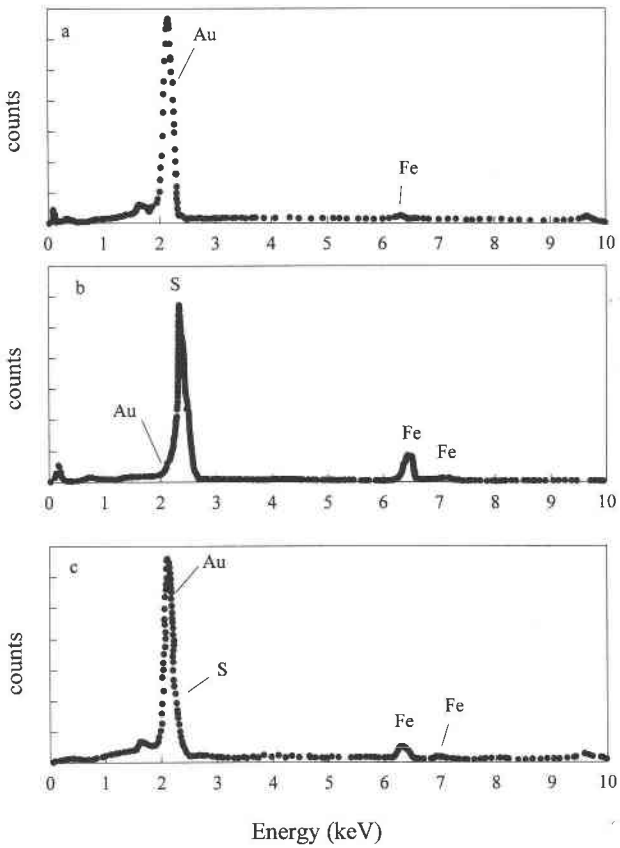

Figure 6. EDXA analysis of reacted Au bisulfide reacted pyrites. Figures 6a and 6b correspond to Figure 5 (**a**) large crystal and (**b**) region below crystal, on small crystals. The scan (**c**) corresponds to the growths in Figure 5c.

reaction conditions for pyrite-Au interactions in chloride solution (Mycroft et al. 1995; Scaini et al. 1997). Aside from the obvious difference in the oxidation state of the Au in the two systems, the key difference lies in the strength of the complex. Au can be viewed as a soft acid and as such will bond more strongly with a soft base such as SH^- than a hard base such as Cl^-. Renders and Seward (1989a) summarized the stability constants for a host of linear XMX complexes where M = Au, Ag and then X = Cl, Br, SCN, I, H_2NCSNH_2, S_2O_3, SH, and CN (order of increasing stability of the complex). The stability of the $Au(SH)_2^-$ complex is approximately 20 orders of magnitude larger than for $AuCl_2^-$. As a result of this, we expect to observe more Au^{1+} species on the mineral surface in the SH^- system, because the complex dissociates to a lesser extent upon adsorption onto the pyrite surface.

Acknowledgments

The authors thank the National Science and Engineering Council of Canada (NSERC) for funding of this work. The authors also thank the staff at Surface Science Western for their technical assistance.

References cited

Benning, L.G. and Seward, T.M. (1995) AuHS°-An important gold-transporting complex in high temperature hydrosulfide solutions. In Kharaka and Chudaev, Eds., Water-Rock Interaction, p. 783–786. Balkema.

——— (1996) Hydrosulfide complexing of Au(I) in hydrothermal solutions from 150–400 °C and 150–1500 bar. Geochimica et Cosmochimica Acta, 60(11), 1849–1871.

Berndt, M.E., Buttram, T., Earley, D., III, and Seyfried, W.E., Jr. (1994) The stability of gold polysulfide complexes in aqueous sulfide solutions: 100 to 150 °C and 100 bars. Geochimica et Cosmochimica Acta, 58(2), 587–594.

Buckley, A.N., Kravets, I.M., Shchukarev, A.V., and Woods, R. (1994) Interaction of galena with hydrosulfide ions under controlled potentials. Journal of Applied Electrochemistry, 24, 513–520.

Cardile, C.M., Cashion, J.D., McGrath, A.C., Renders, P., and Seward, T.M. (1993) ^{197}Au Mössbauer study of Au_2S and gold adsorbed onto As_2S_3 and Sb_2S_3 substrates. Geochimica et Cosmochimica Acta, 57, 2481–2486.

DiCenzo, S.B., Berry, S.D., and Hartford, E.H., Jr. (1988) Photoelectron spectroscopy of single size Au clusters collected on a substrate. Physical Review, B38(12), 8465–8468.

Gammons, C.H. and Barnes, H.L. (1989) The solubility of Ag_2S in near-neutral aqueous sulfide solutions at 25 to 300 °C. Geochimica et Cosmochimica Acta, 53, 279–290.

Gammons, C.H. and Bloom, M.S. (1993) Experimental investigation of the hydrothermal geochemistry of platinum and palladium: II. The solubility of PtS and PdS in aqueous sulfide solutions to 300 °C. Geochimica et Cosmochimica Acta, 57, 2451–2467.

Hayashi, K. and Ohmoto, H. (1991) Solubility of gold in NaCl- and H_2S-bearing solutions at 250–350 °C. Geochimica et Cosmochimica Acta, 55, 2111–2126.

Hayashi, K., Sugaki, A., and Kitakaze, A. (1990) Solubility of sphalerite in aqueous sulfide solutions at temperatures between 25 and 240 °C. Geochimica et Cosmochimica Acta, 54, 715–725.

Kucha, H., Stumpfl, E.F., Plimer, I.R., and Köck, R. (1994) Gold-pyrite association-result of oxysulfide and polysulfide transport of gold? Transactions of the Institution of Mining and Metallurgy. Applied Earth Science, 103, B197–B205.

Lawrance, L.M. and Griffin, B.J. (1994) Crystal features of supergene gold at Hannan South, Western Australia. Mineralium Deposita, 29, 391–398.

Leavitt, A.J. and Beebe, T.P., Jr. (1994) Chemical reactivity studies of hydrogen sulfide on Au (111). Surface Science, 314, 23–33.

Mycroft, J.R., Bancroft, G.M., McIntyre, N.S., and Lorimer, J.W. (1995) Spontaneous deposition of gold on pyrite from solutions containing Au (III) and Au (I) chlorides: I. A surface study. Geochimica et Cosmochimica Acta, 59(16), 3351–3365.

Pan, P. and Wood, S.A. (1994) Solubility of Pt and Pd sulfides and Au metal in aqueous bisulfide solutions: II. Results at 200° to 350 °C and saturated vapour pressure. Mineralium Deposita, 29, 373–390.

Renders, P.J. and Seward, T.M. (1989a) The stability of hydrosulfido- and sulfido-complexes of Au(I) and Ag(I) at 25 °C. Geochimica et Cosmochimica Acta, 53, 245–253.

——— (1989b) The adsorption of thio gold (I) complexes by amorphous As_2S_3 and Sb_2S_3 at 25 and 90 °C. Geochimica et Cosmochimica Acta, 53, 255–267.

Scaini, M.J., Bancroft, G.M., Lorimer, J.W., and Maddox, L.M. (1995) The interaction of aqueous silver species with sulfur-containing minerals as studied by XPS, AES, SEM and electrochemistry. Geochimica et Cosmochimica Acta, 59(13), 2733–2747.

Scaini, M.J., Bancroft, G.M., and Knipe, S.W. (1997) AN XPS, AES and SEM study of the interactions of gold and silver chloride species with PbS and FeS_2: Comparison to natural samples. Geochimica et Cosmochimica Acta, 61(6), 1223–1231.

Seward, T.M. (1973) Thio complexes of gold and the transport of gold in hydrothermal ore solutions. Geochimica et Cosmochimica Acta, 37, 379–399.

——— (1993) The hydrothermal geochemistry of gold. In R.P. Foster, Ed., Gold Metallog. Explor. Chapter 2, p. 37–62. Chapman Hall.

Shenberger, D.M. and Barnes, H.L. (1989) Solubility of gold in aqueous sulfide solutions from 150 and 350 °C. Geochimica et Cosmochimica Acta, 53, 269–278.

Tossell, J.A. (1996) The speciation of gold in aqueous solution: A theoretical study. Geochimica et Cosmochimica Acta, 60, 17–29.

Wood, S.A., Pan, P., Zhang, Y., and Mucci, A. (1994) The solubility of Pt and Pd sulfides and Au in bisulfide solutions: I. Results at 25°–90 °C and 1 bar pressure. Mineralium Deposita, 29, 309–317.

Van de Vondel, D.F., Van der Kelen, G.P., Schmidbaur, H., Wolleben, A., and Wagner, F.E. (1977) ESCA study of gold organometallics. Physica Scripta, 16, 367–369.

Manuscript received March 31, 1997
Manuscript accepted November 11, 1997